



Contents lists available at ScienceDirect

Physica A

journal homepage: www.elsevier.com/locate/physa

Nano-pattern stabilization by multiplicative noise

Sergio E. Mangioni¹

IFIMAR, Instituto de Investigaciones Físicas de Mar del Plata (CONICET–UNMdP), Facultad de Ciencias Exactas y Naturales, Universidad Nacional de Mar del Plata, Deán Funes 3350, (B7602AYL) Mar del Plata, Argentina

ARTICLE INFO

Article history:

Received 3 December 2009

Received in revised form 8 January 2010

Available online 16 January 2010

Keywords:

Stabilization by noise

Pattern formation

ABSTRACT

Within the reaction–diffusion framework, a one-component system was confined by means of a multiplicative noise into the attraction basin of a patterning attractor in its (infinite-dimensional) configuration space. In this way, inhomogeneities that otherwise would have been “expelled” from this basin, and subsequently eliminated through the diffusive process, were stabilized. For the present study, a model describing the physics of adsorbed particles on a metallic surface has been used. In particular, an underlying deterministic inhomogeneity-building mechanism was exploited, that acts driven by lateral interactions among the adsorbed particles. This process cannot by itself sustain and stabilize the inhomogeneities, but together with the contribution of a particular form of multiplicative noise, it is able to confine the system into the region of configuration space where this mechanism is enabled, hence stabilizing the pattern. Although the proposal could be applied to more general situations, for the particular model studied here we have found that nanopatterns that without the indicated noise source would be eliminated by diffusion, under its effect can grow and be stabilized.

© 2010 Elsevier B.V. All rights reserved.

1. Introduction

The last few decades of the twentieth century have witnessed the change in the role of fluctuations in organized systems from a disordering factor towards its present counterintuitive constructive role [1–3]. Among all the possible *noise-induced phenomena*, noise-induced phase transitions are among the most surprising and interesting examples. These can be divided into two classes. The first case to be studied was explained in terms of a noise-induced short-time instability in the local dynamics, collectively sustained in the long time limit by the spatial coupling [4–8]. These ordering phase transitions are characterized for being reentrant with the noise intensity. Initially it was erroneously assumed that the zero-dimensional models exhibiting noise-induced transitions [9] were not able to show any interesting behavior when coupled. However, Ibañes et al. [10–12] have found a second class of noise-induced phase transitions showing that it was not so. They introduced an illustrative generic model that describes a relaxational dynamics in a free-energy functional, with kinetic coefficients depending on the field, and subject to a Gaussian white noise whose multiplicative factor, in order to fulfill the fluctuation–dissipation relation, was the square root of this coefficient. Several differences can be pointed out between both cases: (a) in the 2nd case, at short times, the disordered phase is stable, (b) through the calculation of the exact stationary probability distribution, which is possible in the 2nd case, it can be seen that the disordered phase is destabilized at long times, giving rise to more ordered solutions, (c) for the 2nd case, a transition (although not a phase transition) *also* happens in zero-dimensional cases, (d) the transitions, that for the 1st case are reentrant, are not in the 2nd, but rather they become more ordered as the noise intensity increases.

E-mail address: smangio@mdp.edu.ar.

¹ Member of CONICET, Argentina.

Both physical contexts have been used to study pattern formation [3]. For the purposes of this study, it is the second class of noise-induced ordering phase transitions that matters. On this question, some illustrative works have been reported [13–16]. They exhibit an equation like the one in Refs. [10–12], taking a similar local potential to build the free energy, but replacing the traditional diffusive term (Fick's law) by the Swift–Hohenberg one. They also consider an appropriate form for the kinetic coefficient for each potential. In this way the resulting system is expelled from the disordered phase due to the multiplicative noise, and a competition is introduced between two length scales by means of the Swift–Hohenberg operator, which generates a morphological instability.

There are systems that present underlying inhomogeneity-building mechanisms. These remain hidden by a nonlinear dynamics that drives the system toward attractors located in a region of the configuration space where such mechanisms become innocuous. In other words, these only act for field configurations outside the attraction basin of these attractors. Hence, when the system is forced into those configurations the mechanism becomes activated, and an inhomogeneity grows and develops. Nevertheless, the system reacts by pushing the inhomogeneity outside of this region, where it is eliminated by the diffusion process, and the system is driven toward the basin of the non-patterning attractor. Such mechanisms are based on the action of a functional potential $U[\phi(x)]$ that stimulates order, acting against the diffusion process. An example of such a mechanism is the attractive lateral interactions among adsorbates on metallic surfaces [17–19]. These generate an effect that gathers together the adsorbates, opposing the diffusion process, although they are unable to build by themselves an inhomogeneity that is sustained in time. Such an effect can be modeled with a potential that averages the effect of the lateral interactions on an adsorbate located in a given position.

The objective of this work was to explore the possibility that the system be confined in the constructive region of the field by means of an appropriate multiplicative noise. This way, by avoiding the inhomogeneity being expelled from this region, it would become a stable solution of the system. The noise would confine it by competing against the deterministic forces that expel it from the constructive region. Here it will be shown that this is in fact possible, and it will be exemplified using the model reported in Refs. [17–21].

The paper is organized as follows. In Section 2, the proposal is justified and explained. In Section 3, this proposal is applied to the peculiar case of attractive lateral interactions among adsorbates on a metallic surface. In Section 4, an alternative is presented to that outlined in the previous section. Finally, the conclusions are presented in the last section.

2. Description, analysis and justification of the proposal

Let us consider a generic one-dimensional system, characterized by a positive field $\phi(x, t)$, where x denotes the position and t the time. This system is subjected to a nonlinear force $Q(\phi)$ with at least one attractor ϕ^s , and a diffusion process with coefficient D . It is also subject to an attractive functional potential $U[\phi(x)]$ which generates a current opposing the diffusive effect. If we allow such a current to be affected by prefactors depending on the field, it can be modeled by the expression

$$J = DG(\phi) \frac{\partial U}{\partial x}, \quad (1)$$

where $G(\phi)$ is a positive function indicating such prefactors. Note that within the present framework, the above mentioned attractors are located in a region of configuration space that is completely governed by both the nonlinear force and the diffusive process. This means that in this region, J cannot compete with these processes. With all these ingredients, the dynamics of this system is described by

$$\frac{\partial}{\partial t} \phi(x, t) = Q(\phi) - \frac{\partial}{\partial x} \left[DG(\phi) \frac{\partial U}{\partial x} \right] + D \frac{\partial^2 \phi}{\partial x^2}. \quad (2)$$

The same physics can be exhibited in terms of a reaction–diffusion equation with field-dependent diffusion coefficient. For that end we define

$$\epsilon = \frac{\partial_x U}{\partial_x \phi},$$

which by construction depends on the inhomogeneity profile. If in particular, the pattern is approximately harmonic, such a dependence is expected to be captured through the propagation wave number k . With this definition, the evolution Eq. (2) reads

$$\frac{\partial}{\partial t} \phi(x, t) = Q(\phi) + \frac{\partial}{\partial x} \left[D_{\text{eff}} \frac{\partial \phi}{\partial x} \right], \quad (3)$$

where $D_{\text{eff}} = DD^*$, with $D^* = 1 - \epsilon G(\phi)$. Consistent with the proposed constructive mechanism, ϵ is positive. In the above expression, it is evident that the effect of such a mechanism opposes that of diffusion.

When the constructive mechanism dominates over the diffusive one, D_{eff} can be negative. This effective diffusion coefficient shows the competition between these two opposed forces: the constructive impulse represented by J , opposing the homogenizing effect driven by the true diffusive current. Therefore, for an inhomogeneity to grow and develop it is necessary that D_{eff} be negative. In this way, the ordering forces overcome the disordering ones. This happens in a certain

region of the configuration space and does not guarantee the stability of the arising pattern, as the attractor (or the nearest one if there are more than one) located outside this region will attract the pattern, and then the inhomogeneity will be eliminated by diffusion. Finally, the system will be stabilized in this attractor.

Is it possible that random fluctuations succeed in avoiding this process of elimination of the inhomogeneities gestated in the constructive region of the field? Here, an affirmative answer is given. A Gaussian white noise with an appropriate multiplicative factor can generate other attractors (different from the ones predicted by the deterministic model) which have the peculiarity of being located in the region where D_{eff} is negative. Moreover, and at a fundamental level, this same noise can prevent the pattern being expelled from the constructive region of the field. Finally, without ceasing for this reason to compete with the new attractors, the pattern can be stabilized for a certain window of values of the wave number k .

An important step that brings us near this conclusion is to rewrite Eq. (3) in the form corresponding to a model with relaxational dynamics in a free-energy functional $\mathcal{F}[\phi(x)]$ with a field-dependent kinetic coefficient $\Gamma(\phi)$ and then, in order to fulfill a fluctuation–dissipation relation [10–12], to add to this dynamics, a white noise with a multiplicative factor $\sqrt{\Gamma(\phi)}$. Hence, Eq. (3) takes the form

$$\frac{\partial \phi}{\partial t} = -\Gamma(\phi) \frac{\delta \mathcal{F}[\phi(x)]}{\delta \phi(x)} + \sqrt{\Gamma(\phi)} \eta(x, t), \quad (4)$$

where η is a Gaussian white noise with zero mean and correlation $\langle \eta(x, t) \eta(x', t') \rangle = 2\sigma^2 \delta(x - x') \delta(t - t')$. What is relevant here is to select the appropriate kinetic coefficient, since this determines the multiplicative factor of the noise. The strategy is to confine the system in the constructive region of the field. Since the boundary of this region is defined by the zeros of $D_{\text{eff}}(\phi)$, it is reasonable to build $\Gamma(\phi)$ starting from $D_{\text{eff}}(\phi)$. A form according to the aims is to take $\Gamma(\phi) = 1/|D_{\text{eff}}(\phi)|$. On one hand, the noise intensity is infinite on the boundary separating the constructive region ($D_{\text{eff}} < 0$) from those regions where the inhomogeneities are eliminated ($D_{\text{eff}} > 0$). On the other hand, it decays when the field moves away from this boundary, becoming irrelevant in comparison with the deterministic dynamics. (This will depend on the function $G(\phi)$.) With this choice, the noise is expected to move the field away from this boundary, forcing the system to remain on one side or the other of it. Then, if the system is located in the constructive region it will be confined there, therefore being able to generate and stabilize a pattern.

Although the explicit form of the functional $\mathcal{F}[\phi(x)]$ is irrelevant to the objectives of this work, for this choice of kinetic coefficient it adopts the form

$$\mathcal{F}^{\pm}[\phi(x)] = \int_{-L}^L dx \left\{ - \int_0^{\phi} d\phi |D_{\text{eff}}| Q(\phi) \pm \frac{1}{2} D_{\text{eff}}^2 (\partial_x \phi)^2 \right\},$$

where the $+$ sign corresponds to $D_{\text{eff}} > 0$, while the $-$ sign corresponds to $D_{\text{eff}} < 0$. Here, periodic boundary conditions at $x = \pm L$ are considered, $2L$ being the system's size.

$P_{\text{st}}[\phi]$, the exact stationary probability distribution corresponding to Eq. (4) satisfies [10–12,16,22]

$$P_{\text{st}}[\phi] \sim \exp(-\mathcal{F}_{\text{eff}}^{\pm}/\sigma^2),$$

where the effective potential is

$$\mathcal{F}_{\text{eff}}^{\pm}[\phi(x)] = \mathcal{F}[\phi(x)] - \lambda \int_{-L}^L dx \ln(|D_{\text{eff}}|).$$

Here λ is a (renormalized) parameter proportional to σ^2 . The most probable solutions correspond to the minima of $\mathcal{F}_{\text{eff}}^{\pm}[\phi(x)]$, which can be found by solving [16,22]

$$\frac{\partial \phi}{\partial t} = - \frac{1}{|D_{\text{eff}}|} \frac{\delta \mathcal{F}_{\text{eff}}^{\pm}[\phi(x)]}{\delta \phi(x)}, \quad (5)$$

which explicitly reads

$$\frac{\partial}{\partial t} \phi(x, t) = Q(\phi) \pm \frac{\lambda}{D_{\text{eff}}^2} \frac{d}{d\phi} D_{\text{eff}}(\phi) + \frac{\partial}{\partial x} \left[D_{\text{eff}} \frac{\partial \phi}{\partial x} \right], \quad (6)$$

the $+$ sign corresponding again to $D_{\text{eff}} > 0$, while the $-$ sign corresponds to $D_{\text{eff}} < 0$.

As can be observed, the average effect of this multiplicative noise adds to the nonlinear force as $\pm \frac{\lambda}{D_{\text{eff}}^2} \frac{d}{d\phi} D_{\text{eff}}(\phi)$.

Nevertheless, such an effect can be expressed independently of the choice of the kinetic coefficient as $-\lambda \frac{d\Gamma(\phi)}{d\phi}$.

In Eq. (6) it can be seen that the noise term effectively imposes an infinite wall among the above mentioned regions. Namely, a wall capable of confining the system in the constructive region of the field. Nevertheless, in order to show it more clearly, it is useful to illustrate it in a specific case. In the following section, these ideas will be applied to the case of attractive lateral interactions among particles adsorbed on a metallic surface.

3. Attractive lateral interactions on metallic surfaces

We consider a one-dimensional monolayer model, which was described and founded in detail in Refs. [17–22] and that is expressed in the form of a kinetic mean-field equation. Only one class of particles were considered. Those particles can be adsorbed, desorbed, can diffuse and fundamentally interact amongst themselves. It is precisely this last property that sustains the underlying constructive mechanism. The field was characterized by adopting a continuous description of the surface. This was divided into small elementary areas, each containing a large number of sites. Thus, the field $\phi(x, t)$ was defined as the fraction of the sites inside each area containing adsorbates (coarse graining). Therefore $\phi(x, t)$ varies between 0 and 1.

It was assumed that the lateral interactions are substratum-mediated and that their range can extend from several Angstroms to several nanometers [23]. The small parameter used in this model is the inverse of the number of lattice sites inside the area reached by the interaction radius. From here, the referred kinetic mean-field equation is generally applicable when the attractive interactions extend over many lattice sites.

These attractive lateral interactions produce a strong local bond $U[\phi(x)]$, whose mean-field effect can be calculated from $u(r)$, the interaction potential between two adsorbates. Here x expresses the localization of the adsorbate and r the distance between two of the interacting adsorbates. For $u(r)$ it was proposed that

$$u(r) = -\frac{u_0}{\sqrt{\pi}r_0} \exp[-r^2/r_0^2], \quad (7)$$

the parameter u_0 being the interaction strength and r_0 its mean interaction range. Hence $U[\phi(x)]$ can be obtained as

$$U[\phi(x)] = \int u(x-x')\phi(x')dr'. \quad (8)$$

Hence, the adsorbate is affected by a force $F = -\frac{\partial U}{\partial x}$ that induces a speed $v = \frac{D}{k_b T} F$ (Einstein's relation). Since these can only move through free places we have a factor $1 - \phi$, in this example the prefactor (introduced before in a general way) takes the form $G(\phi) = \frac{\phi(1-\phi)}{k_b T}$. Then, by defining $\epsilon^* = \frac{\epsilon}{k_b T}$, the corresponding nondimensional effective diffusion coefficient can be expressed as $D^* = 1 - \epsilon^*\phi(1 - \phi)$. For a harmonic inhomogeneity, $\epsilon^* = \epsilon_0 \exp[-r_0^2 k^2/4]$, $\epsilon_0 = \frac{u_0}{k_b T}$ being a measure of the interaction strength weighted against the mean kinetic energy of the adsorbate. Here the factor $w^* = \exp[-r_0^2 k^2/4]$ illustrates the effect of the field's inhomogeneity on the current produced by the lateral interactions. It can be seen that, when $r_0 \rightarrow 0$, $\epsilon^* \rightarrow \epsilon_0$ and it is positive for attractive lateral interactions.

The last ones also affect the desorption process. Their rate constant decreases because the effect of the previous ones. Let $k_{d,0}$ be the rate constant in the absence of lateral interactions. Then in their presence, this constant is characterized by

$$k_d(x) = k_{d,0} \exp\left[-\frac{U}{k_b T}\right].$$

In addition, the adsorption process is described as $k_a p(1 - \phi)$, where k_a is the sticking coefficient and p the partial pressure (kept constant) of the gas phase. The factor $1 - \phi$ appears because the particles can only be adsorbed on free sites (monolayer model). Therefore the nonlinear force, constituted by the adsorption and desorption processes, is written as

$$Q(\phi) = k_a p(1 - \phi) - \phi k_{d,0} \exp\left[-\frac{U}{k_b T}\right].$$

It is observed that this model has all the ingredients needed in Eq. (6). In order to write out the corresponding deterministic equation (that is, before incorporating the noise) as one of dynamic relaxation in an energy functional it was considered that D^* does not depend explicitly on x (a) in the limit $r_0 \rightarrow 0$ (if $r_0 \ll 2\pi/k$, $\epsilon^* \simeq \epsilon_0$), (b) for harmonic solutions ($\epsilon^* = \epsilon_0 w^*$), and (c) in a weak form, for quasi-harmonic solutions. This obviously restricts the validity of the proposal. Nevertheless, in the next section it will be shown that similar effects can be caused by adopting another form of the kinetic coefficient that does not depend on the position.

Finally, introducing the forms peculiar to this model into Eq. (6) and proposing the change of variables $\tau = tk_{d,0}$, its average dynamics is expressed by

$$\frac{\partial}{\partial \tau} \phi = Q_b(\phi) \pm \frac{\lambda_a \epsilon^* (2\phi - 1)}{D^{*2}} + L_{\text{dif}}^2 \frac{\partial}{\partial x} \left[D^* \frac{\partial \phi}{\partial x} \right] \quad (9)$$

where

$$\begin{aligned} Q_b(\phi) &= \alpha(1 - \phi) - \phi e^{-\frac{U}{k_b T}}, \\ \alpha &= \frac{k_a p}{k_{d,0}}, \\ \lambda_a &= \frac{\lambda}{D k_{d,0}}, \end{aligned}$$

and $L_{\text{dif}} = \sqrt{D/k_{d,0}}$ is a diffusion length associated to desorption when $\epsilon_0 \rightarrow 0$ (zero-range lateral interaction limit).

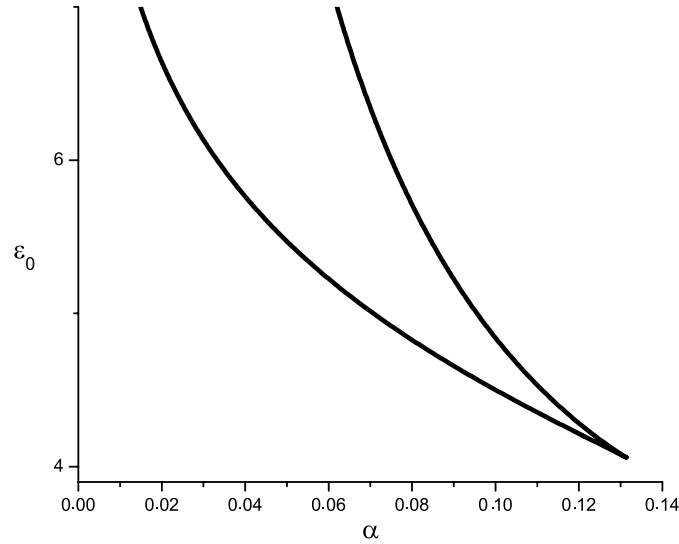


Fig. 1. Bifurcation diagram: the region between the lines that converge in the cusp corresponds to the coexistence of two phases.

$D^*(\phi)$ is a parabola with minimum at $\phi = 0.5$. If $\epsilon^* < 4$, the ordering impulse caused by the attractive lateral interactions always yields to the diffusion process, since $D^*(\phi)$ is positive for the whole domain of the field (range of $\phi = [0 - 1]$). But for $\epsilon^* > 4$, $D^*(\phi)$ is negative in the central region of this domain (around $\phi = 0.5$). It is in this region where the above mentioned constructive mechanism can play its role (recall that ϵ^* depends on k .) In particular, for the possible homogeneous solutions, this condition becomes $\epsilon_0 > 4$.

The homogeneous solutions of the deterministic system are obtained from $Q_b(\phi) = 0$. When one of the roots falls inside the constructive region ($D^*(\phi) < 0$) this is an unstable solution that points out the existence of other two stable ones located in the domain where the diffusion process is strong ($D^*(\phi) > 0$). Otherwise the deterministic system presents only a homogeneous solution. The corresponding bifurcation curve is presented in Fig. 1.

When the noise with its prefactor is added, a new dynamics is introduced, in which the walls indicated in the previous section are evidenced by means of the infinities produced when $D^*(\phi) = 0$. Fig. 2 plots the effective nonlinearity $Q_{\text{eff}}^{\pm}(\phi)$ vs ϕ , with

$$Q_{\text{eff}}^{\pm}(\phi) = Q_b(\phi) \pm \frac{\lambda_a \epsilon^* (2\phi - 1)}{D^{*2}}$$

for a particular case with $k = 0$, whereas Fig. 3 plots the corresponding potential $V_p^{\text{NL}}(\phi)$ vs ϕ . In both of them, two new attractors are exposed, besides the two ones imposed by the deterministic dynamics. The new ones, of stochastic origin, are located in the central area of the field, between the two walls, where D^* is negative. Meanwhile, the attractors of deterministic origin lie on the other side of the walls, where D^* is positive. All this can only happen if $\epsilon_0 > 4$. As already mentioned, this condition makes it possible that D^* becomes negative on a certain central region of the field. The latter means that the ordering effect of the current due to the lateral interactions dominates over the diffusive current. Therefore, on one hand the noise sustains two new homogeneous phases that, on the other hand, can be destabilized by an inhomogeneous perturbation.

It is clear that this ordering phase transition (two attractors without noise, four attractors with noise) cannot occur for zero-dimensional models, since the chosen kinetic coefficient is the inverse of the diffusion coefficient. Nevertheless, if the diffusion term is removed, but keeping the kinetic coefficient (a different physical case), such a transition can occur. As happens for the transitions of the second class mentioned in the introduction, the Stratonovich drift in this model has a form opposed for long times to the one for short times. This can be easily seen through the standard short-time approximation. A simple calculation gives

$$\frac{\partial}{\partial \tau} \phi_m = \alpha(1 - \phi_m) - \phi_m e^{-\epsilon_0 \phi_m} \mp \frac{\lambda_a \epsilon_0 (2\phi_m - 1)}{D_0^{*2}}, \quad (10)$$

where ϕ_m is the first statistical moment and $D_0^* = 1 - \epsilon_0 \phi_m(1 - \phi_m)$; the $-$ sign applies for $D_0^* > 0$ and the $+$ sign for $D_0^* < 0$, just the opposite of Eq. (9). Although the Stratonovich drift modifies the homogeneous solutions, it does not destabilize them. Although this was observed through a linear stability analysis, it can be more clearly seen by plotting the nonlinearity at a short time $Q_{\text{eff}}^{\text{ST}}(c)$ as a function of the field. The corresponding curve is shown in the Fig. 4. In this curve it becomes noticeable that whereas the attractors of deterministic origin maintain the negative slope (a sign of stability), the opposite occurs for those of stochastic origin, which are stable over a long time.

It is convenient that the parameter λ_a (which measures the noise intensity) be very small, because this way the noise affects only where it should. That is to say, it will build the walls, but it will not compete with the deterministic dynamic far

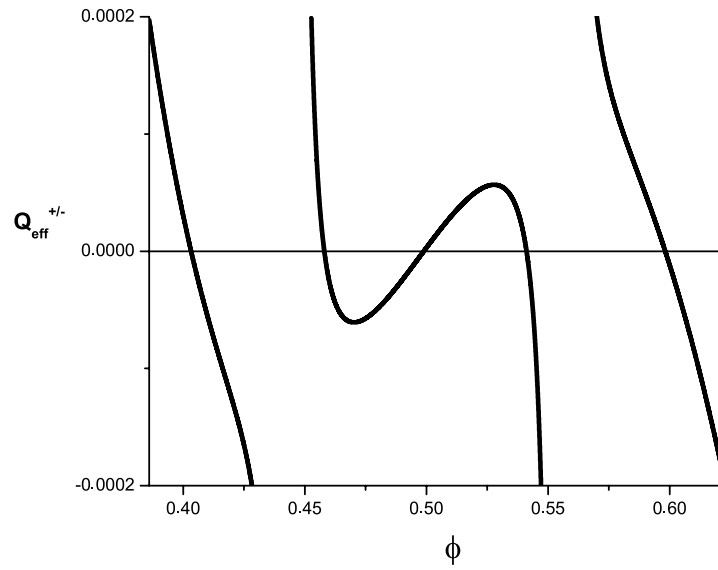


Fig. 2. Non-linearity $Q_{\text{eff}}^{\pm}(\phi)$ vs field ϕ . Parameters $\alpha = 0.132$, $\epsilon_0 = 4.05$ and $\lambda_a = 10^{-8}$. Two attractors of stochastic origin (between the two walls) and another two of deterministic origin (located on the other side of the walls) can be observed.

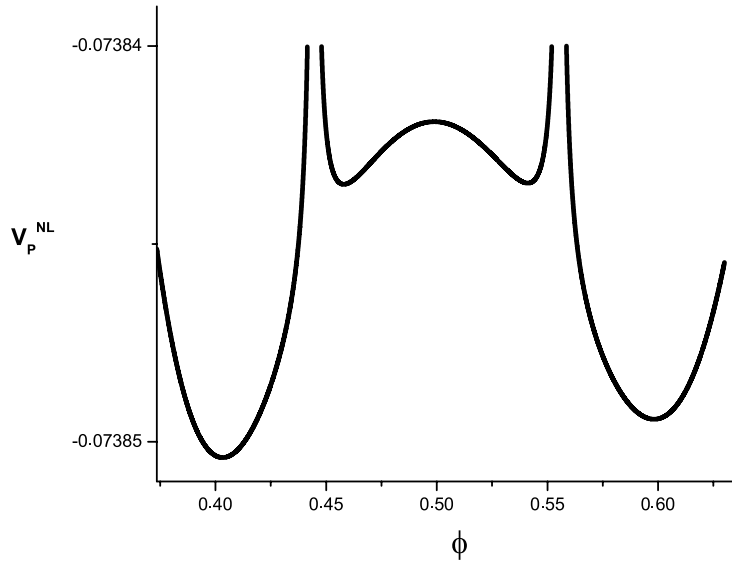


Fig. 3. Potential corresponding to non-linearity $V_P^{\text{NL}}(\phi)$ vs field ϕ . Parameters $\alpha = 0.132$, $\epsilon_0 = 4.05$ and $\lambda_a = 10^{-8}$. Here too, two attractors of stochastic origin (between the two walls) and another two of deterministic origin (located on the other side of the walls) can be observed.

from them. Nevertheless, the above mentioned transition also happens for larger noise intensities. One of the characteristics of this type of transition is that they are not reentrant.

In order to prove that those solutions can be destabilized by an inhomogeneous perturbation, a linear stability analysis was carried out. To that end, the homogeneous solution was perturbed with

$$\delta\phi(x, \tau) = \delta\phi_k + \delta\phi_p \exp(\Omega_k \tau) \exp(ikx),$$

$\delta\phi_p$ being sufficiently small so that all the non-linear terms are negligible. Here $\delta\phi_k$ is a homogeneous perturbation that depends on k , introduced to compensate the modification introduced at zero order by the inhomogeneity (D^* varies with k). The main result of this linear stability analysis is that Ω_k is indeed positive for a window of values of k . More specifically, Ω_k is always real and the unstable modes are not oscillatory. The situation is similar to the classic Turing instability in activator–inhibitor systems: Ω_k has a single maximum, and changes its sign just at the border of the instability for a certain wave number k_0 . This can be observed in the corresponding mathematical expression

$$\Omega_k = -\alpha - \Delta(1 - \epsilon^* \phi^s) - L_{\text{dif}}^2 k^2 D_s^* \pm \lambda_a T_n, \quad (11)$$

with

$$T_n = 2\epsilon^* \frac{D_s^* - \epsilon_0(1 - 2\phi^s)^2}{D_s^{*3}},$$

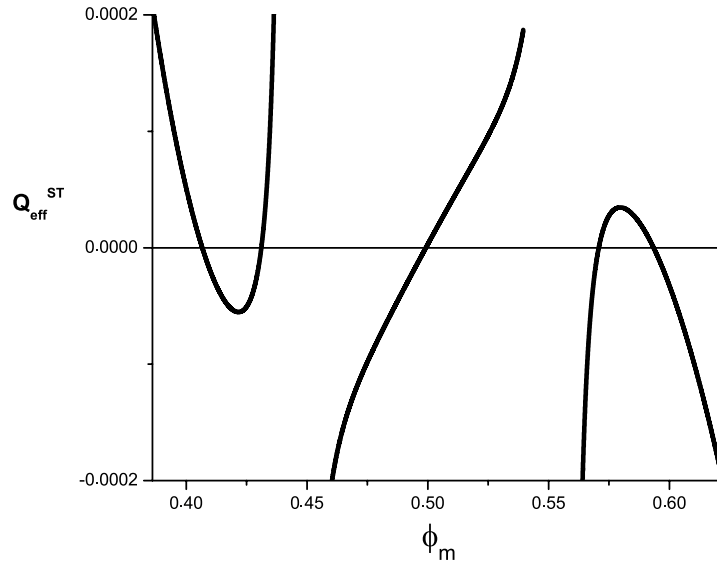


Fig. 4. Short-time non-linearity $Q_{\text{eff}}^{\text{ST}}(\phi)$ vs field ϕ . Parameters $\alpha = 0.132$, $\epsilon_0 = 4.05$ and $\lambda_a = 10^{-8}$. The two attractors of stochastic origin (located between the two walls) are stable at long times, but unstable at short times. On the other hand, the two attractors of deterministic origin (located on the other side of the walls) keep their stability.

$$\begin{aligned} D_s^* &= 1 - \epsilon^* \phi^s (1 - \phi^s), \\ \epsilon^* &= \epsilon_0 w^*, \\ w^* &= \exp[-r_0^2 k^2 / 4], \\ \Delta &= e^{-\epsilon_0 \phi^s}, \end{aligned}$$

with $\phi^s = \phi_0^s + \delta\phi_k$ and ϕ_0^s the stationary homogeneous solution. Here the noise term always stabilizes the homogeneous solution of stochastic origin ($-$), since D_s^* is negative for it.

The relevant role of the noise is only to build the walls, and hence the new homogeneous solutions; but it had a negative influence on the action of destabilizing them with an inhomogeneous perturbation. From the expression (11) it can be seen that the relevant term is $-L_{\text{diff}}^2 k^2 D_s^*$. This is the one that really competes with the attractor (recall that for this c^s it is $D_s^* < 0$). This term increases from 0 with increasing k , but since $-D_s^*$ simultaneously decreases with k , a maximum is reached (the decrease of $-D_s^*$ also affects the noise, pushing the maximum toward smaller k). At this maximum Ω_k crosses the line of the zero toward positive values, indicating that the first mode destabilizes. Therefore, considering that

$$\Omega_k[k, \phi^s(k)] = 0$$

and

$$\partial_k \Omega_k[k, \phi^s(k)] / k = 0,$$

the contour was determined of the region of parameters where an inhomogeneous perturbation can destabilize the homogeneous solution of stochastic origin (the division by k is meant to exclude the trivial solution). Fig. 5 shows the stability curves in the ϵ_0 vs α plane for different noise intensities. Destabilization occurs above the curve, i.e. for larger ϵ_0 . The most open curve corresponds to the largest value of λ_a ; as λ_a decreases, the curves close on themselves, until finally the instability region disappears. This is not a surprise when considering that the smaller the noise intensity, the closer the homogeneous solution comes to the infinite wall ($D^* = 0$); this circumstance makes the attractor push the system more intensely toward this solution; and then, the lateral interactions do not achieve its destabilization. For a real situation on the other hand, the walls are not infinite and therefore, starting from a certain minimum λ_a , they will cease to effect the system.

A fact that requires attention is that all the curves show a coincident minimum. This can be clarified when considering that the homogeneous solutions of stochastic origin arise when D_{eff} becomes negative. Since D_{eff} has a minimum at $\phi_0^s = 0.5$, the new homogeneous solution will arise around this value, with $\epsilon_0 = 4$. The localization of this coincident minimum (ϵ_0^{cusp} , α^{cusp}) corresponds to the cusp at which the two branches of the bifurcation diagram meet (see Fig. 1) and is independent of the values of λ_a .

It is interesting to notice that given $\epsilon^* = \epsilon_0 w^*$, the current due to the lateral interactions is largest at $\phi = 0.5$, since the product $\phi(1 - \phi)$ of the covering by the number of free sites attains its maximum. From the calculations it is observed that $\phi^s \approx 0.5$ only when the minimum of D_s^* is approximately zero, which happens if $\epsilon^* \approx 4$. Considering this, it can be appreciated that next to the cusp, the wave number k_0 of the first mode destabilizing ϕ_0^s is smaller than any other corresponding to ϵ_0 and α far from ϵ_0^{cusp} and α^{cusp} . It then becomes clear why the lowest transition point lies in this cusp, with $\epsilon^* \approx \epsilon_0 \approx 4$ and therefore with $w^* = \exp[-r_0^2 k_0^2 / 4] \approx 1$, which indicates that k_0 should be sufficiently small as to justify this relation. In other words, keeping ϵ_0 constant, $-D_s^*$ as evaluated in $\phi^s = 0.5$ is larger than for any other value of ϕ^s ; therefore, for this value of the field, Ω_k reaches its maximum more quickly. Conversely, as we move away from α^{cusp} ,

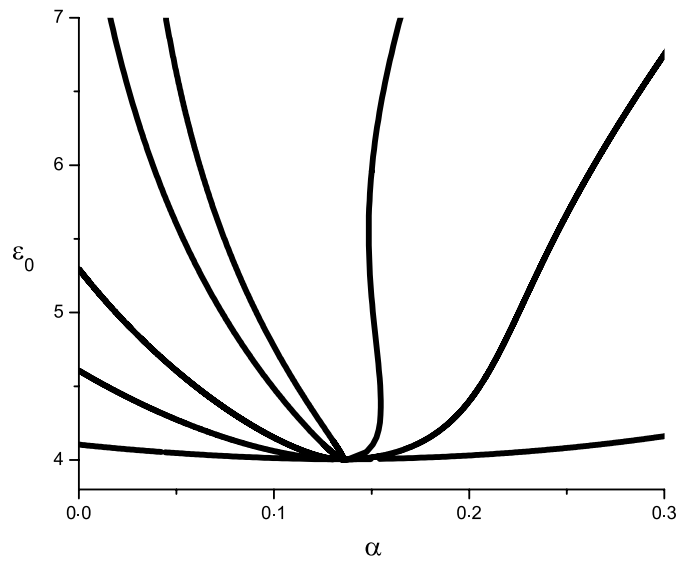


Fig. 5. Stability curves for different noise intensities. Above them (i.e. for larger ϵ_0), the homogeneous solutions of stochastic origin can be destabilized by an inhomogeneous perturbation. All the curves show a coincident minimum, the most open one corresponding to $\lambda_a = 10^{-7}$. Then they close in on themselves, $\lambda_a = 10^{-8}$, 2.5×10^{-9} , 5×10^{-11} . The midrange $r_0 = 0.001L_{\text{diff}}$.

k_0 increases monotonically. This is due to the fact that ϕ^s also moves away from 0.5 and then the current due to lateral interactions decreases. For this reason, it is also necessary to increase ϵ_0 so that the instability boundary be crossed. For those values of α far from α^{cusp} , ϕ^s varies significantly with λ_a , which strongly affects the stability curves.

For the process of destabilization to occur, it is important that r_0 be small and the diffusion length large enough. On one hand, the factor L_{diff} potentiates the destabilization effect produced by the lateral interaction current ($D_s^* < 0$); whereas a small r_0 maintains the effective diffusion coefficient negative until large enough values of k so that the destabilizing force dominates over the attractor (see Eq. (11)). For $D_s^* > 0$, a larger L_{diff} helps in faster “washing” of the inhomogeneities; but for $D_s^* < 0$, it helps in building them. Also, for r_0 larger than a certain critical value, a small value of k suffices to make $D_s^* > 0$; and then, the homogeneous solution can be never destabilized (the constructive effect dies out for r_0 larger than this critical value). For a given r_0 , this effect also imposes a lower bound to the first destabilizing mode. As it has already been argued, this minimum happens in the region of the cusp. The smaller r_0 and the larger L_{diff} , the larger will the minimum k_0 be. For the type of metallic surfaces that this model describes, $r_0 \sim 1 \text{ nm}$ [23] and $L_{\text{diff}} \sim 1 \mu\text{m}$ [24,25]. With these values, the k_0 minimum calculated is around $10 \mu\text{m}^{-1}$, a fact that leads us to speak of nanostructures (wavelength between 1 nm and 1 μm).

To prove that those nanopatterns can truly emerge and be stabilized, the corresponding attractors were perturbed with a harmonic profile of very small amplitude. Points were selected inside and outside the instability region. Then the evolution of the perturbation was followed with both dynamics, the stochastic one (Eq. (4)) and that of the most probable pattern (Eq. (9)). For the points located outside the instability region, it was observed that a small perturbation is quickly homogenized. But for those points located inside this region, the perturbation grows until it is stabilized into a pattern of approximately harmonic shape and with a wavelength in the range of the nanometers. In Fig. 6, an example of these solutions is shown. The thick line is the most probable pattern (Eq. (9)) and the thin line is the one obtained with the stochastic dynamics (Eq. (4)). For the range of variation of the position x , the already mentioned values $r_0 \sim 1 \text{ nm}$ [23] and $L_{\text{diff}} \sim 1 \mu\text{m}$ [24,25] were taken as reference. The two lines between which the most probable pattern is located indicate the two noise walls. It can be observed that the pattern calculated with the stochastic dynamics overcomes these walls. This is due to the fact that a wall of finite height was used in the simulation of the stochastic process. Therefore the stochastic force can deliver enough energy to the system so that part of the pattern overcomes this wall. This does not mean that the pattern is destabilized, since for this to happen the whole pattern should overcome the wall. This did not occur in any of the simulated cases. The noise, acting on certain points of the profile, offers a resistance capable of balancing the force caused by the deterministic attractor. The effect is evident when the noise is turned off while the pattern is reaching the stationary state. It can be observed that the senses of growth are reverted. The attractor begins to attract the pattern and this slowly diminishes its amplitude.

Following the evolution of the most probable patterns, it was observed that when one of the ends of the pattern approaches a noise wall before reaching the stationary state, the field ceases to grow. Nevertheless, the amplitude of the pattern continues to grow. It happens as if when its amplitude grows, the pattern were pushed back from this wall. Then, the stationary state is finally reached. Fig. 7 shows this effect. The curves in thin lines correspond to very early stages of the evolution, while the one in a thick line shows the stationary state (this is reached at a much longer time, yet longer than the one sufficient to obtain the appreciable shape in the graph).

For the calculations to be correct, one must be cautious to select a sufficiently small time interval not to allow the field to cross the wall for numerical reasons. The abrupt slope that the non-linear force presents around the wall can produce

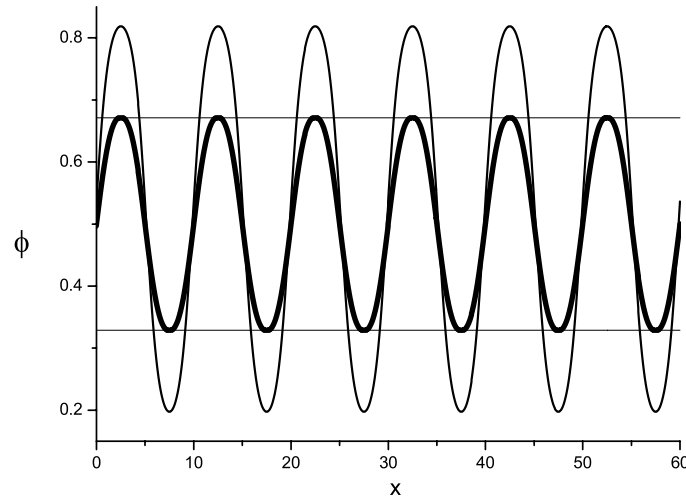


Fig. 6. Field $\phi(x)$ vs position x , measured in nanometers. The thick line corresponds to the most probable pattern. The thin line corresponds to a simulation of the stochastic process. $\alpha = 0.1$, $\epsilon_0 = 5$, and $\lambda_a = 2 \cdot 10^{-9}$. The midrange $r_0 = 0.001 \mu\text{m}$. The two lines between which the most probable nanopattern is located indicate the two noise walls.

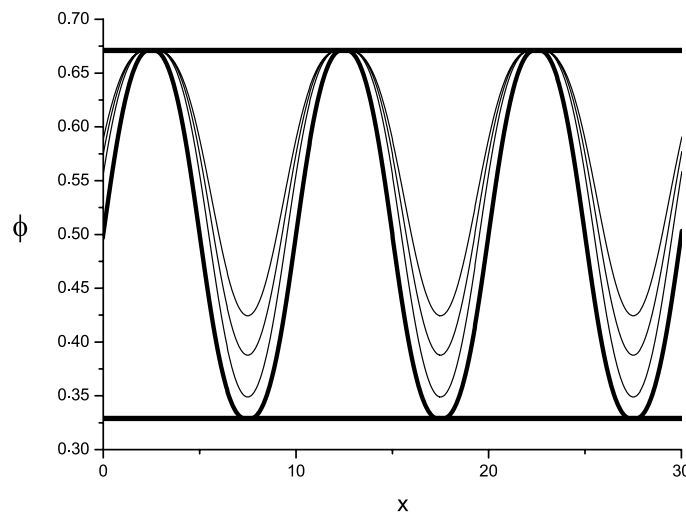


Fig. 7. Long-time evolution of a nanopattern, before reaching the stationary state. The thin-line curves correspond to very early stages of evolution, while the one in a thick line displays the steady state (this is reached at a much longer time, yet longer than the one sufficient to obtain the appreciable shape in a graph.) The position x is measured in nanometers. $\alpha = 0.1$, $\epsilon_0 = 5$, and $\lambda_a = 2 \cdot 10^{-9}$. The midrange $r_0 = 0.001 \mu\text{m}$. The two lines between which the nanopatterns are located indicate the two noise walls.

discretization errors. Nevertheless this fact does not destabilize the pattern, since the part that is maintained inside the constructive area by the walls of noise sustains it. Something similar happened when the simulation of the stochastic process was carried out. Fig. 8 shows an example of such a circumstance. As is observed when comparing with Fig. 6, this pattern is superimposed on the one calculated for the stochastic process.

The lack of fluctuations in the calculated pattern with the stochastic process could be a surprise: the standard deviation of the average pattern is not appreciable in the shown profiles. Nevertheless, it has already been mentioned that the stochastic force affects only a very small neighborhood of the boundary between the domain of the diffusive processes and that of the constructive one, the rest being at the “mercy” of the deterministic forces. For quite larger noise intensities ($\lambda_a \sim 10^{-2}$), such fluctuations begin to arise.

4. Other forms of kinetic coefficient and multiplicative noise

As was outlined in Section 2, our objective is to confine the system in the constructive region of the field. Although it was shown that this can be done by confining it in this region, between infinite walls induced by the noise, the particular form proposed here presents certain problems that make its study difficult. On one hand real walls are of finite height, making it possible that the system crosses them. On the other hand, the walls are very narrow, which forces the use of a very small time step and therefore long computing times. Another option that has proven viable is that instead of generating new attractors, the noise displaces those of deterministic origin toward the constructive region. In this way, the deterministic attractor changes its role as a “decoy” (it attracts the pattern toward the region where the diffusive process eliminates it)

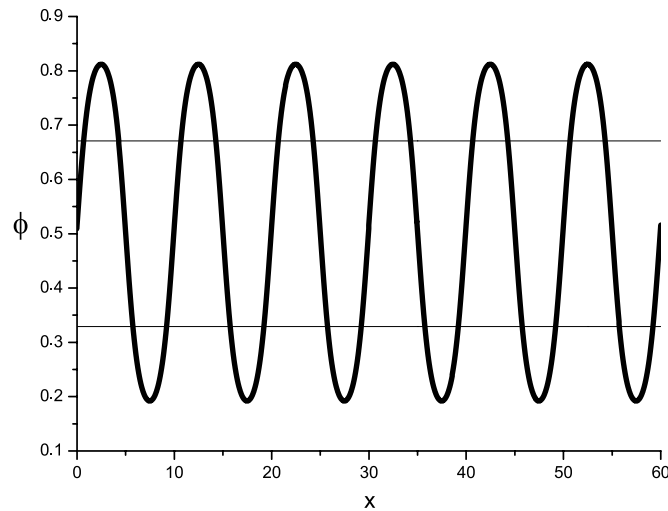


Fig. 8. Idem as in Fig. 6, but with a time step 10 times larger. The two lines between which the nanopattern is located indicate the two noise walls. It can be seen that the nanopattern surpasses both walls. The position x is measured in nanometers. $\alpha = 0.1$, $\epsilon_0 = 5$, and $\lambda_a = 2 \cdot 10^{-9}$. The midrange $r_0 = 0.001 \mu\text{m}$.

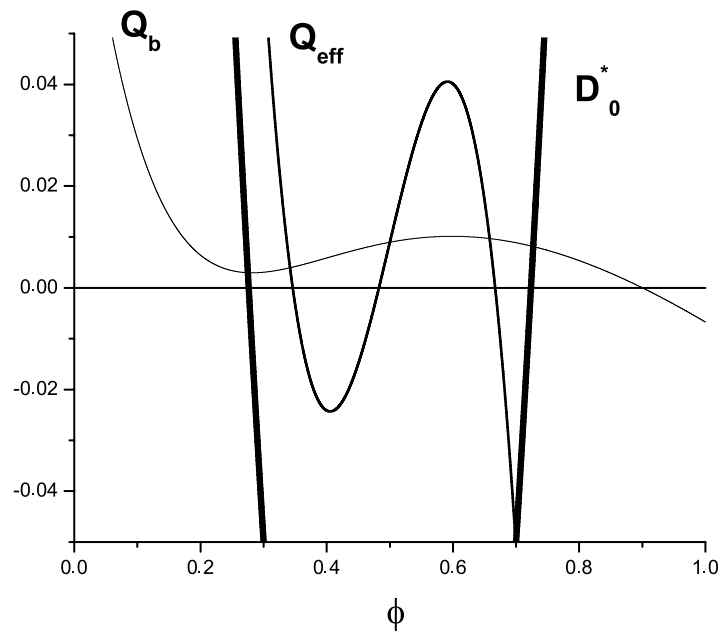


Fig. 9. Non-linearity without and with noise vs ϕ : $\alpha = 0.1$, $\epsilon_0 = 5$, and $\lambda_a = 1$. The thick line plots $D_0^*(\phi)$ vs ϕ .

to that of a “plain competitor” of the constructive process. With this prefactor, and for a range of parameters characteristic of the particular model, as well as inside a certain window of values of k , the attractor always loses. The idea is choosing a kinetic coefficient that provides a high noise intensity in the domain of the diffusive process, and a very low one in the constructive region. In the framework of the example used in the previous section, the following one is proposed

$$\Gamma(\phi) = (\phi - 0.5)^2 D_0^* + C,$$

where $D_0^* = 1 - \epsilon_0 \phi(1 - \phi)$ and C is a constant that guarantees that $\Gamma(\phi)$ is always positive or zero. Fig. 9 shows the effect of this multiplicative noise on the effective non-linearity, and compares it with the deterministic non-linearity. Also shown is the curve D_0^* vs ϕ that delimits both domains, that of the constructive mechanism and that of the diffusion process. As is observed, not only has the deterministic attractor moved toward the constructive region but rather another attractor has been created inside it. Any inhomogeneous perturbation of these attractors is thus expected to give rise to a pattern. Also for this case a linear stability analysis was made, showing that such attractors are unstable under an inhomogeneous harmonic perturbation, inside a certain window of values of the wave number k . Fig. 10 shows, for different values of the noise intensity, the corresponding stability diagrams superimposed on the bifurcation ones.

Contrary to the previous case, here the noise modifies the bifurcation diagram. The widening of the region with two attractors is apparent in Fig. 9 as well. Also, the shape of the curve that limits the instability resembles this diagram, showing

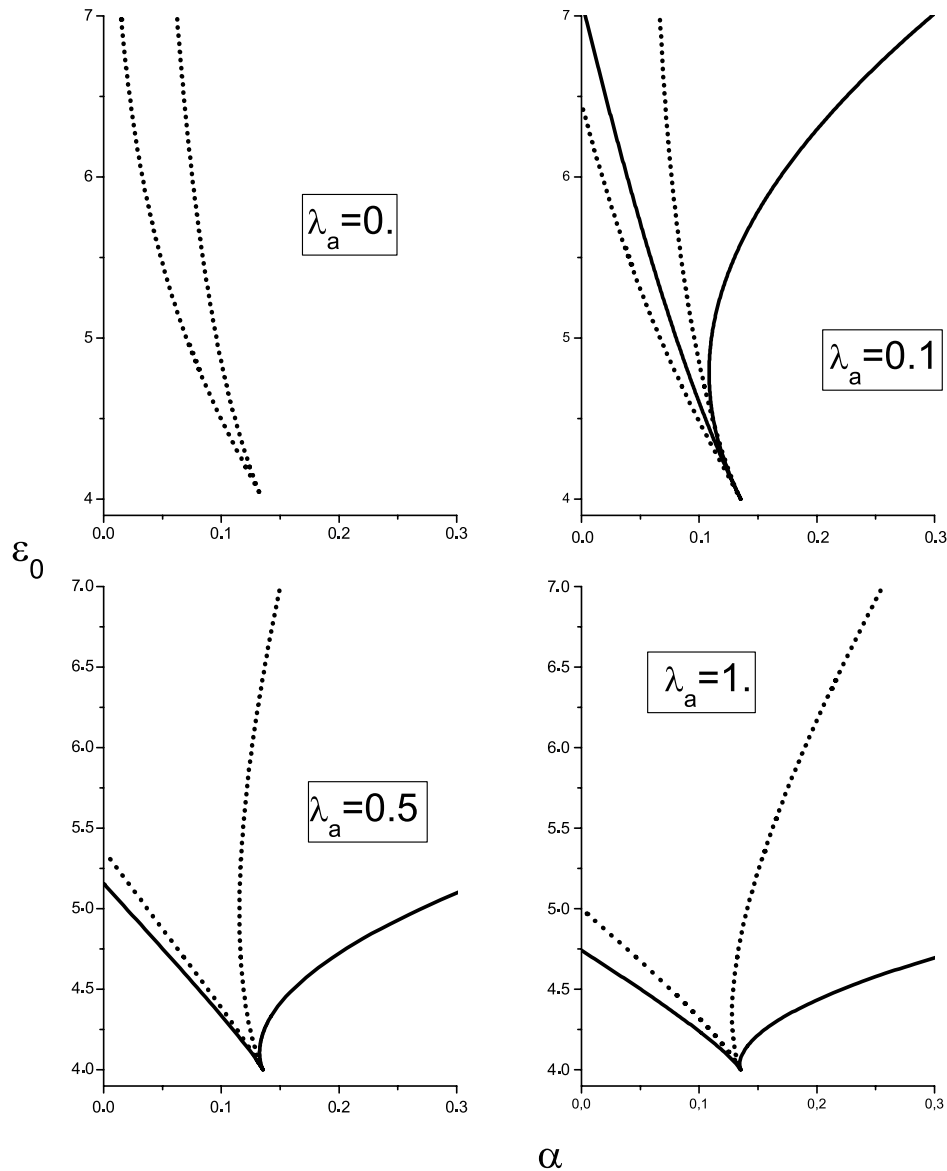


Fig. 10. Stability (solid line) and bifurcation (dot line) curves for different noise intensities. $\Gamma(\phi) = (\phi - 0.5)^2 D_0^* + C$, where $D_0^* = 1 - \epsilon_0 \phi(1 - \phi)$ and the constant C guarantees that $\Gamma(\phi)$ be always positive or zero. The midrange $r_0 = 0.001 L_{\text{diff}}$.

a cusp at the same point as the bifurcation curve. Comparing with Fig. 5, it is seen that this particular class of noise does not only enable a parameter region where a pattern can arise and be stabilized, but also that the form of its multiplicative factor strongly conditions the boundary of this region.

Also, as before, patterns were sought among the solutions of Eq. (9). One of them is shown in Fig. 11, superimposed on another one, calculated with the same values of parameters but obtained with numerical simulations of the stochastic process (Eq. (4)). As can be observed, the differences between both patterns are not appreciable. This is due to the fact that the noise is only imposed in the domain of the diffusive process. Contrarily, in the constructive region where the pattern emerges and is stabilized, the noise is almost unnoticed by the deterministic process. It only acts confining the system in this region. In this sense, the overlap with the pattern obtained with the previous coefficient $\Gamma(\phi)$ is also remarkable. This can be appreciated by observing Fig. 6. Beyond the particular introduced noise, the pattern is built by the deterministic dynamics because the noise only confines the system in the constructive domain. Clearly, if the noise intensity is increased too much, such characteristics are lost and the patterns not only begin to fluctuate but also to depend on the multiplicative noise factor.

Finally, all these patterns are also nanostructures like the ones shown in the previous case.

5. Conclusions

This work considers a physical system showing an underlying constructive mechanism, which is not enough to sustain the built order. Such a mechanism plays a role in a region of the field from which the system is expelled by the forces acting on it. Here it has been shown that and how the system can be confined in the constructive region of the field by an appropriate

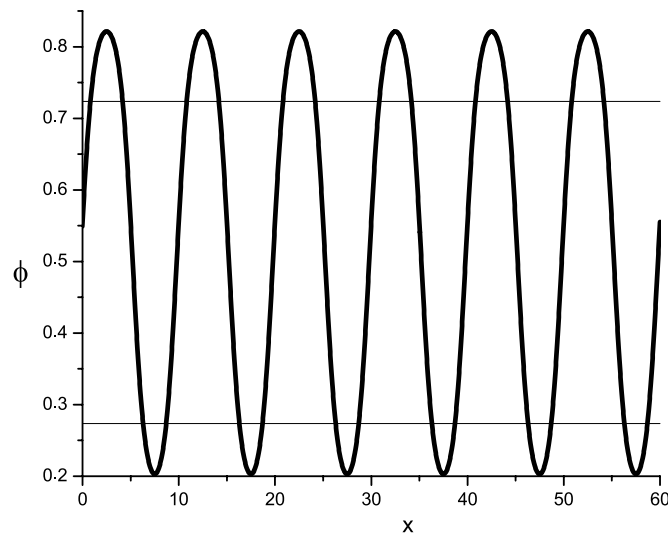


Fig. 11. Field $\phi(x)$ vs position x , measured in nanometers. The thick line corresponds to a simulation of the stochastic process. The thin line corresponds to the most probable pattern. $\alpha = 0.1$, $\epsilon_0 = 5$, and $\lambda_a = 1$. The midrange $r_0 = 0.001 \mu\text{m}$. The two horizontal lines indicate the limit between constructive and diffusive domains.

multiplicative noise. Such a noise can be internal, since it is constructed in a such way to satisfy the fluctuation–dissipation relation; but it can also be incorporated from outside. Although it has been exemplified on a particular model in which the referred constructive role rests on the attractive lateral interactions among particles adsorbed on a metallic surface, this study transcends this fact, being applicable to any other model of similar characteristics. Only a mechanism to build order is required that can be assimilated as the field-depending part of an effective diffusion coefficient. Hence, the pattern can be rewritten like the already typical reaction–diffusion equation with variable diffusion coefficient. The existence of the underlying constructive mechanism is expressed in this coefficient by means of a negative part that opposes the diffusion process. Then, this equation is mapped into a dynamic relaxation equation with field-depending kinetic coefficient. The choice of such a coefficient is decisive for the sought confinement, since its square root is the multiplicative factor of the noise in question.

The effective diffusion coefficient represents a bid among the constructive effects and those that disorder, any of them being able to win. Hence, there will be regions in configuration space where one effect dominates over the other and necessarily, a boundary between these regions. The boundary will correspond to the value of the field that makes the effective diffusion coefficient zero. Taking advantage of this circumstance, the corresponding kinetic coefficient was designed after the diffusion one. The noise intensity was sought to be very large in the region of the field intended to be avoided, and very small elsewhere for the effects of the noise being negligible in comparison to the deterministic dynamics. In the example, two different kinetic coefficients were tried. Both caused the expected effect, so evidencing the versatility of the proposal. The patterns that are eliminated by diffusion in the absence of the noise, subsist confined in the constructive region of the field in the presence of noise. This was shown both analytically and through simulations of the stochastic process. On one hand, a linear stability analysis revealed that the attractors can be destabilized by an inhomogeneous perturbation, their parameter region being clearly identified. On the other hand, the corresponding most probable patterns were identified and compared with those obtained from numerical simulations of the stochastic processes. The coincidences between both patterns was remarkable. Yet more remarkable was the extremely low standard deviation of the profiles calculated with the stochastic process. This was due to the proposed noise structure, that only has appreciable effects in the domain of the diffusive process where the field is absent after being expelled by the noise.

As a relevant aside, it was shown that the combined effect of the attractive lateral interactions and this multiplicative noise gives rise to the formation of stable nanostructures on adsorbed metallic surfaces. In the absence of this type of noise, such nanostructures are not viable.

Regarding testing these results in real experiments, it is well known that fluctuations can be introduced in a controlled way [26,27], making possible the design of an experiment to check the general conclusions of this work. Nevertheless, for those referred to the particular model dealt with here, the resolution required to work in such a small-scale lattice has yet not been reached. Also the capacity to observe a pattern whose wavelength is only a few nanometers is limited. The application of photoelectron emission microscopy (PEEM) offers the possibility to observe spatiotemporal nanopatterns of short wavelength with a resolution of the order, or even smaller, than $1 \mu\text{m}$ [28,29]. This leads one to expect that the possibility to observe such nanopatterns is real, and generates the hope that the present paper could stimulate such investigations.

Finally, it is emphasized that these conclusions transcend the particular model on which they have been obtained. It is expected that many physical processes or mechanisms of order generation can be written as a contribution opposing the true diffusion process. If this is possible, then it is also possible for a multiplicative noise to confine the system in the constructive region of the field, and in this way promote the generation and stabilization of patterns.

Acknowledgements

The author thanks R.R. Deza and H.S. Wio for fruitful discussions and the critical reading of the manuscript. He also acknowledges financial support from CONICET (PIP 5072/05) and UNMdP (EXA425/08) of Argentina; as well as the support of AECID, Spain, through Projects A/013666/07 and A/018685/08.

References

- [1] L. Gammaitoni, P. Hänggi, P. Jung, F. Marchesoni, *Rev. Modern Phys.* 70 (1998) 223.
- [2] P. Reimann, *Phys. Rep.* 361 (2002) 57.
- [3] F. Sagués, J.M. Sancho, J. García-Ojalvo, *Rev. Modern Phys.* 79 (2007) 829.
- [4] C. Van den Broeck, J.M.R. Parrondo, R. Toral, *Phys. Rev. Lett.* 73 (1994) 3395.
- [5] C. Van den Broeck, R. Toral, R. Kawai, *Phys. Rev. E* 55 (1997) 4084.
- [6] S. Mangioni, R. Deza, H.S. Wio, R. Toral, *Phys. Rev. Lett.* 79 (1997) 2389.
- [7] S. Mangioni, R. Deza, R. Toral, H.S. Wio, *Phys. Rev. E* 61 (2000) 223.
- [8] S.E. Mangioni, R.R. Deza, H.S. Wio, *Phys. Rev. E* 63 (2001) 041115.
- [9] W. Horsthemke, R. Lefever, *Noise Induced Transitions*, Springer, Berlin, 1984.
- [10] M. Ibañes, J. García-Ojalvo, R. Toral, J.M. Sancho, *Phys. Rev. Lett.* 87 (2001) 020601.
- [11] O. Carrillo, M. Ibañes, J. García-Ojalvo, J. Casademunt, J.M. Sancho, *Phys. Rev. E* 67 (2003) 046110.
- [12] J. Buceta, K. Lindenberg, *Phys. Rev. E* 69 (2004) 011102.
- [13] J.M.R. Parrondo, C. Van den Broeck, J. Buceta, F.J. de la Rubia, *Physica A* 224 (1996) 153.
- [14] J. Buceta, M. Ibañes, J.M. Sancho, K. Lindenberg, *Phys. Rev. E* 67 (2003) 021113.
- [15] K. Wood, J. Buceta, K. Lindenberg, *Phys. Rev. E* 73 (2006) 022101.
- [16] B. von Haeften, G. Izs, S. Mangioni, A.D. Sánchez, H.S. Wio, *Phys. Rev. E* 69 (2004) 021107.
- [17] A. Mikhailov, G. Ertl, *Chem. Phys. Lett.* 238 (1994) 104.
- [18] D. Batogkh, M. Hildebrandt, F. Krischer, A. Mikhailov, *Phys. Rep.* 288 (1997) 435.
- [19] M. Hildebrand, A.S. Mikhailov, *J. Phys. Chem.* 100 (1996) 19089.
- [20] S.B. Casal, H.S. Wio, S. Mangioni, *Physica A* 311 (2002) 443–457.
- [21] M. Hildebrandt, M. Kuperman, H.S. Wio, A.S. Mikhailov, G. Ertl, *Phys. Rev. Lett.* 83 (1999) 1475.
- [22] S.E. Mangioni, H.S. Wio, *Phys. Rev. E* 71 (2005) 056203.
- [23] M. Hildebrand, A.S. Mikhailov, G. Ertl, *Phys. Rev. Lett.* 81 (1998) 2602(4).
- [24] M. Hildebrand, A.S. Mikhailov, G. Ertl, *Phys. Rev. E* 58 (1998) 5483(11).
- [25] M. Hildebrand, *Chaos* 12 (1) (2002).
- [26] Y. Hayase, S. Wehner, J. Küppers, H.R. Brand, *Phys. Rev. E* 69 (2004) 021609.
- [27] S. Wehner, Y. Hayase, H.R. Brand, J. Küppers, *J. Phys. Chem. B* 108 (2004) 14452.
- [28] P. Hoffmann, S. Wehner, D. Schmeisser, H.R. Brand, J. Küppers, *Phys. Rev. E* 73 (2006) 056123.
- [29] K. Fukumoto, W. Kuch, J. Vogel, F. Romanens, S. Pizzini, J. Camarero, M. Bonfim, J. Kirschner, *Phys. Rev. Lett.* 96 (2006) 097204.